Published online 28 June 2018

Nucleic Acids Research, 2018, Vol. 46, No. 15 ***7747–7756***
doi: 10.1093/nar/gky579

The transcription-coupled DNA repair-initiating protein CSB promotes XRCC1 recruitment to oxidative DNA damage

Hervé Menoni[1,2,*,†], Franziska Wienholz[1,†], Arjan F. Theil[1], Roel C. Janssens[1], Hannes Lans[1], Anna Campalans[3,4], J. Pablo Radicella[3,4], Jurgen A. Marteijn[1] and Wim Vermeulen[1,*]

[1]Department of Molecular Genetics, Oncode Institute, Cancer Genomics Netherlands, Erasmus MC, Dr. Molewaterplein 40, 3015 GD Rotterdam, The Netherlands, [2]Laboratoire de Biologie et Modélisation de la Cellule (LBMC) CNRS, ENSL, UCBL UMR 5239, Université de Lyon, Ecole Normale Supérieure de Lyon, 69007 Lyon, [3]CEA, Institute of Cellular and Molecular Radiobiology, F-96265 Fontenay aux Roses, France and [4]UMR967 CEA, INSERM, Universités Paris-Diderot et Paris-Sud, F-92265 Fontenay aux Roses, France

Received October 20, 2017; Revised June 07, 2018; Editorial Decision June 13, 2018; Accepted June 22, 2018

ABSTRACT

Transcription-coupled nucleotide excision repair factor Cockayne syndrome protein B (CSB) was suggested to function in the repair of oxidative DNA damage. However thus far, no clear role for CSB in base excision repair (BER), the dedicated pathway to remove abundant oxidative DNA damage, could be established. Using live cell imaging with a laser-assisted procedure to locally induce 8-oxo-7,8-dihydroguanine (8-oxoG) lesions, we previously showed that CSB is recruited to these lesions in a transcription-dependent but NER-independent fashion. Here we showed that recruitment of the preferred 8-oxoG-glycosylase 1 (OGG1) is independent of CSB or active transcription. In contrast, recruitment of the BER-scaffolding protein, X-ray repair cross-complementing protein 1 (XRCC1), to 8-oxoG lesions is stimulated by CSB and transcription. Remarkably, recruitment of XRCC1 to BER-unrelated single strand breaks (SSBs) does not require CSB or transcription. Together, our results suggest a specific transcription-dependent role for CSB in recruiting XRCC1 to BER-generated SSBs, whereas XRCC1 recruitment to SSBs generated independently of BER relies predominantly on PARP activation. Based on our results, we propose a model in which CSB plays a role in facilitating BER progression at transcribed genes, probably to allow XRCC1 recruitment to BER-intermediates masked by RNA polymerase II complexes stalled at these intermediates.

INTRODUCTION

Our genome is constantly challenged by a large number of DNA damaging agents leading to various types of DNA lesions. DNA damage contributes to genome instability and is associated with serious consequences for human health, including cancer, neurodegeneration and ageing (1,2). Reactive oxygen species (ROS) are undesirable byproducts of cells' oxygen consumption and a major source of unavoidable endogenously produced DNA damage. Among the various different types of oxidative DNA lesions, the highly mutagenic 8-oxo-7,8-dihydroguanine (8-oxoG) is one of the most abundant (3,4). In eukaryotic cells, the bifunctional glycosylase 8-oxoG-glycosylase 1 (OGG1) specifically recognizes and excises the 8-oxoG from the sugar backbone leaving an abasic site (5). The DNA chain at this abasic site is subsequently cleaved by either OGG1's intrinsic AP lyase activity that creates 3′α,β-unsaturated aldehyde and 5′-phosphate termini (5) or by AP endonuclease 1 (APE1) which produces 3′-OH and 5′-ribose-phosphate termini. The X-ray repair cross-complementing protein 1 (XRCC1) protein stimulates the APE1 activity to allow efficient processing of the intermediates left by OGG1 (6,7). This proposed complex cascade of events is currently difficult to address *in vivo* partly due to redundant factors that deal with 8-oxoG.

*To whom correspondence should be addressed. Tel: +31 107043194; Fax: +31 107044743; Email: w.vermeulen@erasmusmc.nl or Hervé Menoni; Email: herve.menoni@ens-lyon.fr

†The authors wish it to be known that, in their opinion, the first two authors should be regarded as Joint First Authors.

Present address: Hervé Menoni, Laboratoire de Biologie et Modélisation de la Cellule (LBMC) CNRS, ENSL, UCBL UMR 5239, Université de Lyon, Ecole Normale Supérieure de Lyon, 69007 Lyon, France; Université de Grenoble Alpes/INSERM U1209, CNRS UMR 5309, 38042 Grenoble Cedex 9, France.

Most of the BER factors downstream of the glycosylases are essential for cell viability (2,8). The 70-kDa XRCC1 protein was initially thought to be mainly required for coordinating single-strand DNA break repair (SSBR), by functioning as a non-enzymatic scaffold protein to which several factors involved in sealing the DNA nick are recruited (9,10). Single-strand breaks induce the production of poly ADP-ribose (PAR) chains, catalyzed by the Poly ADP-ribose polymerases 1 or 2 (PARP-1 or PARP-2) enzymes, which are required for recruiting XRCC1 to DNA breaks (11,12). While neither XRCC1 nor parylation are required for BER of 8-oxoG to proceed *in vitro* (13), biochemical studies on DNA with uracil suggested that XRCC1 could direct BER towards the short-patch gap-filling branch (14). *In vitro* experiments on chromatinized templates showed that BER efficiency is not only supported by chromatin remodelers and specific histones chaperons (15,16), but also by XRCC1, which possibly further disrupts or translocates inhibiting nucleosomes (17). With the use of live cell microscopy and locally induced oxidative DNA damage we have previously shown that while XRCC1 recruitment to direct SSBs is dependent on parylation, its relocalization to BER complexes does not require this post-translational modification (18). Moreover, several studies showed that XRCC1 is directly recruited to BER through its interaction with the glycosylases that recognize the damage (7,9,19–21). It is thus likely that for its important function in coordinating BER, XRCC1 is recruited to SSBs originating from BER-intermediates through direct protein-protein interactions rather than only parylated substrates.

In addition, we previously showed that the Cockayne syndrome B protein (CSB) is quickly recruited to oxidative base damage in a transcription-dependent manner, with almost similar kinetics as the OGG1 glycosylase (18,22). CSB is essential for transcription-coupled nucleotide excision repair (TC-NER), a dedicated sub-branch of NER to resolve transcription-blocking DNA lesions (23). Since cells from Cockayne Syndrome (CS) patients were found to be hyper-sensitive to oxidative DNA damage, a role for the CS proteins in the response to oxidized bases has been proposed (24–27). However, whether a dedicated transcription-coupled BER (TC-BER) pathway, analogous to TC-NER, exists has been subject to controversy. The notion that 8-oxoG lesions, which only cause minor helix-distortions (28), do not block RNA polymerase II (RNAPII) elongation unless processed by its specific glycosylase 8-oxoguanine glycosylase (OGG1) (29–31), suggests that if indeed TC-BER exists it is not directly triggered by stalled RNAPII on the oxidative lesions itself as in TC-NER. Further support for transcription-associated processing of BER lesions comes from recent data showing the involvement of the histone-chaperone FACT (facilitates chromatin transcription) in BER (32), which is in line with a previously established role of FACT in TC-NER (33).

To investigate the existence of a transcription-associated BER process, we exploited our recently developed tool to locally inflict different types of DNA lesions and to monitor the subsequent recruitment kinetics of repair factors in living cells. To that aim, we used isogenic cells, which either express CSB or have the *CSB* gene disrupted by CRISPR/Cas9-mediated genome editing. The stable expression of fluorescently tagged BER proteins in those isogenic cells allowed us to directly assess the impact of CSB on the behavior of BER proteins.

MATERIALS AND METHODS

Cell lines, constructs and transfection

The CRISPR/Cas9 genome editing approach was applied to obtain CSB knock out cells. Specific single guide RNA (sgRNA) sequences, targeting introns 2 and 3 of the CSB gene respectively, were cloned in a LentiCRISPRv2 plasmid. The LentiCRISPRv2 plasmid was a gift from Feng Zhang (Addgene plasmid #52961, (34)). The guide sequences are as follows: 5′-GCGAGGGCTGAACGGGA TGG-3′ and 5′-GCTTTGGAAAACTTAAGGGT-3′. To clone these constructs, annealed complementary oligo's with 5′ overhangs were ligated in the BsmB1 digested backbone of the LentiCRISPRv2 plasmid. The correct insert was verified by sequencing. Sv40 immortalized MRC-5 cells were transiently co-transfected with 1 μg of each of the two indicated LentiCRISPRv2 plasmids at 70% cell density on a single well of a 6-well cultured plate using Polyplus Jet-Pei transfection reagent (Westburg). Transfection was carried out according to the manufactures protocol. Transfected cells were selected using 3 μg/ml puromycin for several days. Subsequently, single cells were seeded on a 96-well plate to obtain pure clones and tested for knock out by genotyping and Western blot analysis.

Plasmids pEGFP-N1 and pEYFP-N1 (Clonetech) containing XRCC1-YFP, XRCC1^{L360D}-YFP or OGG1-GFP were described in (18). Fluorescent cDNA fusions were amplified by PCR and subsequently cloned into pLenti CMV Puro (Addgene plasmid #17452; (35)). Third-generation lentiviruses, generated in HEK293T cells, were used to transduce Sv40 immortalized MRC-5 cells and it's isogenic Sv40 immortalized MRC-5 CSB knock-out cells. We further used the Sv40 immortalized human fibroblasts CS1AN (Cockayne syndrome group B-deficient [CS-B]) and HeLa cells. The following constructs were used for transient or stable expression of fluorescently tagged proteins: pOGG1-DsRed, pmCherry-CSB, pXRCC1-EYFP and pXRCC1^{L360D}-EYFP (18). Transient transfections were performed with Fugene6 reagent (Roche), according to the manufacturer's instructions. Stably expressing cells were obtained by using puromycin for 1 week to select for resistant cells. Prior to experiments, all cells were grown in a 1:1 mixture of Ham's F10 and DMEM (Gibco), supplemented with penicillin/streptomycin and 10% FCS at 37°C, in a 5% CO_2 humidified incubator.

Western blot

Cells were lysed in 2× Laemmli sample buffer and were boiled for 5 min. Protein size-fractionation by a 6% SDS–PAGE gel and subsequent electro-transfer to a PVDF membrane (0.45 μm) was accomplished as described (36). Blotting was performed overnight at 4°C, 75 mA in 2× Blot-buffer (50 mM Tris, 384 mM Glycin, 0.02% SDS) without methanol. Blocking of the membranes was accomplished with 3% BSA in PBS for 1 h at room temperature. Membranes were then washed three times with PBS

containing 0.05% Tween and were subsequently incubated with primary antibodies against CSB (E-18, sc-10459, Santa Cruz Biotechnology, Inc., 1:250 in PBS 3% BSA), Tubulin (B512, Sigma-Aldrich, 1:5000 in PBS 3% BSA), or OGG1 (ab12474, Abcam, 1:1000 in PBS 3% BSA) or SFPQ (ab177149, Abcam, 1:2000 in PBS 3% BSA) in combination with Odyssey-compatible secondary antibodies. Western blots were analyzed using the Odyssey CLx Infrared Imaging System (LI-COR Biosciences).

Gentoyping

PCR amplification was used for verifying the deletion of exon 3 in the endogenous CSB gene. 100 ng DNA of each sample was used per PCR reaction. Taq DNA polymerase was purchased from Invitrogen and used according to the manufacturer's instructions. PCR conditions were as follows: 95°C for 3 min, 35× [95°C for 45 s, 60°C for 30 s, 72°C for 2 min], 72°C for 10 min. The primer sequences used are as follows: forward primer: 5′-ggcagtgtcaggtaagcaag-3′, reverse primer: 5′-agttgggatggcagaactga-3′. PCR products were run on an agarose gel containing ethidium bromide. The expected PCR products are: 2.1 kb for exon 3 containing (wild-type CSB) and 210 bp for exon 3 deleted (CSB KO).

Colony survival

MRC-5 and MRC-5 CSB-deficient cells were seeded in triplicate in six-well plates (300 cells/well) and treated with a single dose of UV-C (0–6 J/m^2; 254 nm; Philips TUV lamp) or with a single dose of Potassium Bromide ($KBrO_3$, 0–10 mM) 1 day after seeding. After 7 days, colonies were fixed and stained in 50% methanol, 7% acetic acid and 0.1% Coomassie blue and subsequently analyzed with the Gelcount by Oxford Optronix and appertaining Software (version 1.1.2.0). The survival was plotted after pooling three (UV-C) or two ($KBrO_3$) independent experiments as the mean percentage of colonies detected 1 week after damage treatment compared to the mean number of colonies from the non-treated samples.

Silencing and cell treatments

Small interfering RNAs against CSB (ON-TARGETplus SMART-pool; L-004888-00-0020, Human ERCC6, NM_000124; Dharmacon), targeting OGG1 (On-TARGETplus SMARTpool; L-005147-00, Human OGG1; Dharmacon) or non-targeting (siGENOME NonTargeting D-001210-05-20, Dharmacon) were transfected to cells using Lipofectamine 2000 reagent (Invitrogen), according to the manufacturer's instructions. Silencing in HeLa OGG1-DsRed cell lines with indicated small interfering RNAs was performed using Lipofectamine RNAiMAX reagent (Invitrogen) according to the manufacturer's instructions. Silencing efficiency was determined using western blotting. PARP activity was inhibited with *N*-(6-oxo-5,6-dihydro-henanthridin-2-yl)-*N*,*N*-dimethylacetamide HCl hydrochloride hydrate (PJ-34) purchased from Sigma–Aldrich and used at a concentration of 15 μM (37). Transcription was inhibited with the RNAPII inhibitor 5,6-dichlorobenzimidazole 1-β-D-ribofuranoside (DRB, 100 μM, Sigma-Aldrich) added 2 h prior to the experiment or Actinomycin D (1 μg/ml, Sigma-Aldrich) added 2 h prior to experiment (38).

Microscopic settings, damage induction and FRAP

Images were recorded with different confocal microscopes; Nikon A1, Leica TCS SP5 microscope (with Leica Application Suite) and LSM 510 (Carl Zeiss), all equipped with a 63× Plan-APO (1.4 NA) oil immersion lens. Two days prior to microscopy experiments cells were seeded to full confluency on sterile glass coverslips. During microscopy, cells were examined in normal culture medium maintained at 37°C and 5% CO_2 within a large chamber included in the microscope. Imaging of eGFP, eYFP and DsRed were performed using respectively 488, 514 and 561 nm laser light to excite the chromophores; emitted light was recorded with the respective filters BP505-550, BP530-600 and LP585. Local base damage in a subnuclear area of 2 × 2 μm was induced, as previously described (22). For the induction of direct SSBs a single (1 frame; 2.58 s/frame) 405 nm laser-pulse (corresponding to ∼1 mW) was used. For the induction of oxidative base damage, cells were incubated for 10 min with 10 μM photosensitizer Ro 19-8022 (a kind gift from F. Hoffmann-La Roche, Ltd) and irradiated as described above. Accumulation of DNA repair factors at locally damaged sites was determined by measuring the fluorescent intensity in the damaged area and compared to non-damaged areas of the same size. The measured fluorescence on the damaged area was corrected for background and monitor bleaching, normalized for pre-damage values and averaged. It should be noted that for all the quantitative experiments we have carefully selected cells with comparable expression levels.

Fluorescence recovery after photo-bleaching (FRAP) experiments were performed as previously described (22). In short, the pre-defined damaged and non-damaged subnuclear areas of 2 × 2 μm were illuminated with the respective laser set to 100% laser power for 6 frames (0.032 s/frame) to bleach fluorescent proteins of interest. The subsequent fluorescence recovery was recorded before (100 frames) and after (750 frames) photobleaching, normalized to pre-bleaching values and expressed as mean relative fluorescence intensity.

RESULTS

CSB has no effect on OGG1 immediate recruitment and retention at oxidative DNA damage

We previously established a procedure to measure the recruitment kinetics of OGG1 to locally generated oxidative DNA damage (22). Using that approach we showed that CSB was recruited to these sites in a transcription-dependent manner. Interestingly, the absence of co-recruitment of downstream NER factors suggested that not a full TC-NER reaction was activated at these sites (22). To further explore a possible role of CSB in BER, we measured the recruitment kinetics of OGG1 to local oxidative

DNA damage in the presence and absence of CSB. To that aim we stably expressed OGG1 tagged with GFP in Sv40-immortalized MRC-5 cells. We applied CRISPR/Cas9-mediated genome editing to obtain an isogenic CSB knock-out cell line, in which the absence of CSB was confirmed by PCR and western blotting (Supplementary Figure S1A and B). As expected, those cells have an increased sensitivity to UV-C light exposure (Supplementary Figure S1C) and to oxidative damage (Supplementary Figure S1D). We observed an immediate and fast recruitment of OGG1 to local oxidative DNA damage containing sites in wild-type (wt) cells (Figure 1A and B) in accordance with earlier reports (18). Surprisingly however, the recruitment kinetics of OGG1 in wt and CSB-deficient cells were identical (Figure 1A and B), indicating that CSB is not involved in the immediate glycosylase recruitment. Comparable results were obtained in HeLa cells stably expressing OGG1 fused to DsRed that were depleted for CSB via RNA silencing (Supplementary Figure S1E and G). Together, these data indicate that in different human cells the rapid recruitment of OGG1 to oxidative damage (8-oxoG) is independent of CSB.

We previously reported a faster disappearance of OGG1 accumulation to local oxidative damage in CSB-deficient cells (22). This may suggest that although CSB is not required for the initial OGG1 recruitment, it might be involved in retaining OGG1 at the site of damage. To test this hypothesis, we performed fluorescence recovery after photobleaching (FRAP) experiments on locally induced oxidative damage. In a non-damaged area of wt or CSB-deficient cells, the fluorescent signal quickly recovered after bleaching (Figure 1C), indicative for a freely diffusing protein. The fluorescence recovery was however incomplete when photobleaching was performed at sites of induced oxidative damage in both wt and CSB-deficient cells (Figure 1C), suggesting that a fraction of OGG1 is immobilized (bound) at these sites. We did however not observe a difference in the amount of lesion-bound OGG1 in the absence or presence of CSB. Similar results were obtained in HeLa cells stably expressing OGG1-DsRed in which CSB is knocked down by siRNA (Supplementary Figure S1F and G). Despite the notion that a slower repair of 8-oxoG was observed in CSB-deficient mouse embryonic fibroblasts (MEFs) compared to wild-type littermates MEFs (25), we were not able to unveil differences in the *in vivo* OGG1 binding properties early after damage induction. Since the full repair of 8-oxoG lesions requires several hours (39), it is possible that CSB influences OGG1 binding to a subset of 'difficult-to-repair' oxidative DNA lesions. For example, the immediate targeting of glycosylases to lesions may be impaired due to sequence context, chromatin status or lesions located in close vicinity of each other. However, within our experimental conditions it was not possible, to reveal these subtle differences and to measure binding kinetics at later stages after damage induction. We conclude that OGG1 is rapidly recruited to sites of damage in a CSB-independent manner. This implies that 8-oxoG lesions can efficiently be removed in the absence of CSB and that the formed AP-site is most likely rapidly processed to a SSB in a BER-dependent manner either by the AP-lyase activity of the glycosylase or by APE1.

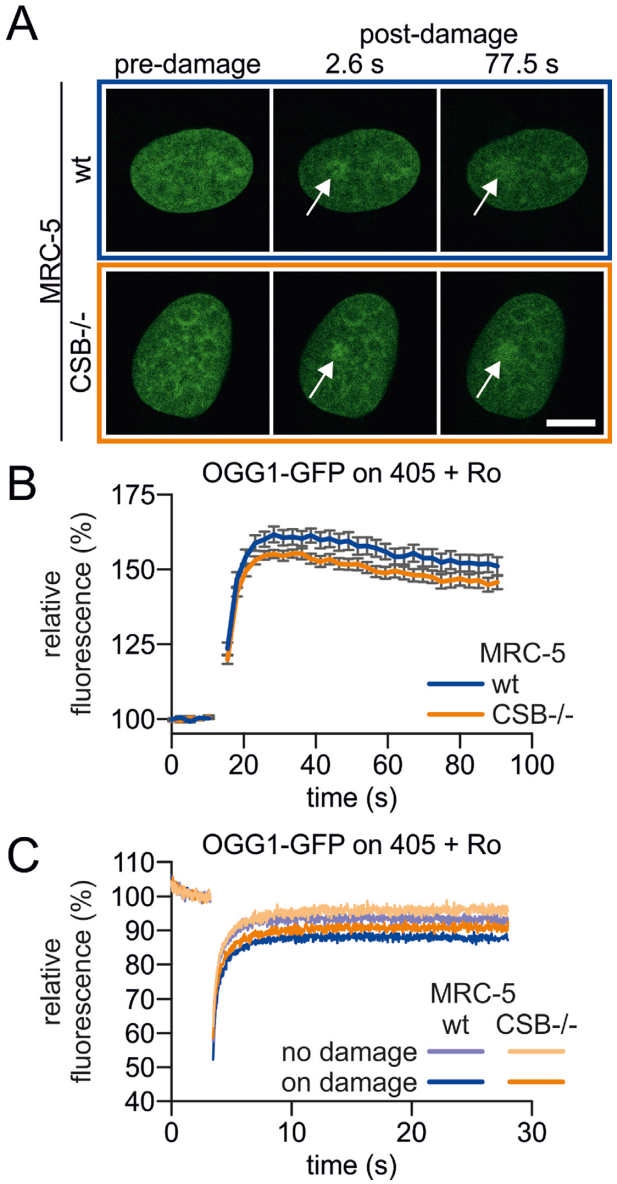

Figure 1. CSB does not affect the recruitment of OGG1 to oxidative DNA damage. (**A**) Representative stills of time-lapse imaging to determine accumulation kinetics of OGG1-GFP in CSB-proficient (upper panel) or CSB-deficient (lower panel) MRC-5 cells at micro-irradiated (405 nm) subnuclear regions, indicated by arrows, in the presence of 10 μM Ro 19-8022 photosensitizer. Scale bar: 7.5 μm. (**B**) Accumulation kinetics of OGG1-GFP at micro-irradiated areas (as shown in A). The mean relative fluorescence intensity is plotted against time in seconds. (**C**) FRAP analysis of OGG1-GFP expressed in CSB-proficient and deficient MRC-5 cells at locally damaged areas (on damage) or at a similar sized area without DNA damage (no damage). For (B) and (C), error bars indicate the SEM of 20 cells of 2 independent, pooled experiments.

CSB facilitates recruitment of XRCC1 to BER-intermediates

Our results show that CSB is not required for the first step of BER, i.e. loading of the glycosylase OGG1. However, CSB-deficient cells have reduced repair rates of 8-oxoG and are hyper-sensitive to oxidative DNA damage, arguing for a role of CSB in a more downstream step of the BER process ((26,27,40,41) and Supplementary Figure S1D). To further

elucidate the role of CSB in BER, we addressed the question whether CSB may be required to facilitate recruitment of XRCC1 to BER. To understand whether CSB influences XRCC1 recruitment to either BER or SSBR, sub-nuclear local DNA damage was induced under two different conditions in cells stably expressing XRCC1-YFP. Firstly, for the induction of mainly direct SSBs (i.e. independent of glycosylases) we employed the 405 nm laser as was reported before (42,43). For simplicity, DNA damage induced with those settings is named 'direct SSBs' (labeled as 405 in figures). Secondly, for the induction of mainly oxidative base damage, cells were pre-incubated with a specific exogenous photosensitizer (Ro 19-8022) prior to 405 nm laser irradiation (22). Results obtained under this condition are labelled 405 + Ro in the figures. Under the latter condition mainly BER-induced SSBs will be formed.

XRCC1-YFP, stably expressed in both CSB-proficient and deficient MRC-5 cells showed an equally robust and rapid accumulation in locally 405 nm laser irradiated areas (direct SSBs) (Figure 2A and B). These data show that CSB is not involved in XRCC1 loading at direct SSBs. Previous studies have shown a strong PARP-dependent recruitment of XRCC1 to direct SSBs (18,43,44). Consistently, the addition of the PARP-inhibitor PJ-34 (37) nearly completely abolished the recruitment of XRCC1 to direct SSBs, which again appeared independent of CSB (Figure 2A, B).

Next, we measured XRCC1 accumulation on BER-induced SSBs generated by 405 nm laser irradiation in the presence of the photosensitizer Ro 19-8022. Pre-treating cells with the PARP-inhibitor PJ-34, allowed us to measure the recruitment of XRCC1 specifically to BER-induced SSBs (Figure 2C and D). Strikingly, under those conditions we now observed a marked CSB-dependency for the recruitment of XRCC1, while active parylation by PARP was not required. When XRCC1-YFP and mCherry-CSB were co-expressed in CSB-deficient cells we find a clear co-localization at the local oxidative damage site (Supplementary Figure S2A), supporting the CSB-dependent XRCC1 recruitment.

The use of PARP inhibitors may result in the accumulation of trapped PARP-1 at the site of damage which may further interfere with BER progression (21). To overcome this potential PARP-inhibitor side effect, we used a mutated XRCC1 (XRCC1^{L360D}-YFP), carrying a point mutation in the BRCT1 domain that abolishes the interaction with PARP-1 and was shown to impede XRCC1 accumulation on direct SSBs (18). As anticipated, no accumulation of the XRCC1^{L360D}-YFP mutant on direct SSBs, in either wt or CSB-deficient cells, was detected (Figure 2E and F). Interestingly however, recruitment of this XRCC1^{L360D}-YFP mutant to BER-intermediates (e.g. BER-induced SSBs) exhibited a strong dependency on CSB (Figure 2G and H). These results were verified in HeLa (CSB-proficient) and CS1AN (CSB-deficient) cells, ruling out a cell type specific effect (Supplementary Figure S1H). These data further corroborate that part of the XRCC1 accumulation on BER-induced SSBs is independent of PARP, but is facilitated by CSB. Previously, it was found that OGG1 expression is reduced in CSB-deficient cells, which may contribute to the reduced XRCC1 recruitment in CSB-deficient cells. However, in our CSB-deficient cells we did not observe any significant OGG1 reduction (Figure 1SG), indicating that XRCC1 recruitment is facilitated by the presence of CSB.

Recruitment of XRCC1 during BER is sensitive to inhibition of transcription

Since CSB recruitment to local oxidative base damage occurs in a transcription-dependent manner (22), we tested whether the recruitment of XRCC1 to BER-induced SSBs is also dependent on transcription. To test this, we used cells expressing the XRCC1^{L360D}-YFP mutant that only accumulates on BER-induced SSBs (Figure 2G and H). Pretreatment of MRC-5 wt cells for 2 h with the transcription inhibitor DRB strongly reduced the accumulation of XRCC1^{L360D}-YFP to locally generated BER-induced SSBs (Figure 3A and B). Similar reduction in accumulation of XRCC1^{L360D}-YFP to local oxidative damage was observed after treatment with the transcription inhibitor Actinomycin-D (Supplementary Figure S2B and C). This transcription-dependent accumulation of XRCC1 was reproduced in HeLa cells expressing XRCC1^{L360D}-YFP (Figure 3C and Supplementary Figure S2C and D). In contrast, the CSB-independent accumulation of dsRed tagged OGG1 appeared independent of transcription (Figure 3D).

DISCUSSION

Based on our results we propose a model in which CSB facilitates the recruitment of XRCC1 to transcription complexes that are stalled at BER intermediates generated during oxidative DNA damage repair (Figure 4, lower panels). We speculate that the combined presence of CSB and XRCC1 assist downstream BER steps. Our previous work (22) already showed a transcription-dependent recruitment of CSB to 8-oxoG. Surprisingly however, targeting of the initiating glycosylase OGG1 to those lesions appeared independent of CSB and transcription (Figure 1A and B), arguing for a transcription-dependent role of CSB beyond initial damage recognition. This observation is in line with earlier observations that the minor helix distorting 8-oxoG lesions do not interfere with RNAPII elongation (29,31,45) and would thus not require CSB. In contrast bulky DNA lesions (e.g. UV-induced photoproducts) that block RNAPII elongation trigger the recruitment of CSB to initiate classical TC-NER (46). However, BER-intermediates (e.g. AP-sites, SSBs) generated either by bifunctional glycosylases (such as OGG1) or as a consequence of APE1 action and not yet fully processed by downstream BER steps may create a local structural DNA disturbance at which RNAPII complexes can stall and trigger CSB recruitment to facilitate XRCC1 binding (47). Surprisingly however, upon OGG1 depletion by siRNA we did not observe a significant reduction of the XRCC1 recruitment (Supplementary Figure S2E and F). The absence of an effect of OGG1 depletion is likely explained by (partly) redundant glycosylases that compensate for the loss of OGG1 (48), or that the remaining OGG1 after incomplete knock down is sufficient to initiate BER. In addition, 405 nm laser-irradiation in the presence of Ro 19-8022 will induce, next to the predominant 8-oxoG lesions, also other types of oxidative base damage which will be targeted by other glycosylases and thus also create BER-intermediates. Nevertheless, the notion from our previous

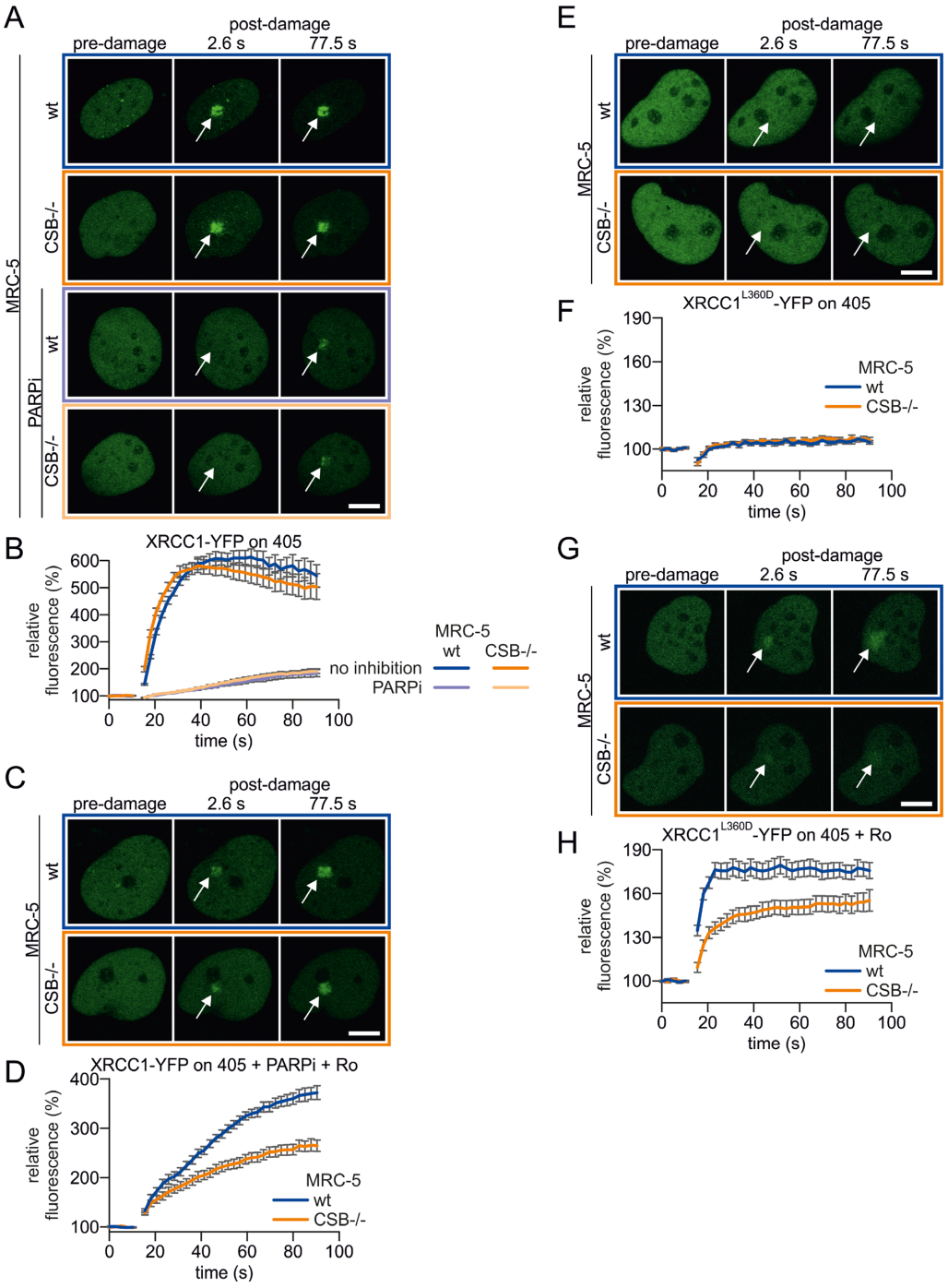

Figure 2. CSB facilitates recruitment of XRCC1 to BER-induced single strand breaks. (**A**) Representative stills of time-lapse imaging to determine accumulation kinetics of XRCC1-YFP in CSB-proficient or CSB-deficient MRC-5 cells on direct SSBs (405 nm laser micro-irradiated regions, indicated by arrows) in the absence (upper two panels) or presence of 15 μM PJ-34 to inhibit PARPs (lower two panels). (**B**) Accumulation kinetics of XRCC1-YFP at micro-irradiated areas (as shown in A). The mean relative fluorescence intensity is plotted against time in seconds. (**C**) Representative stills of time-lapse imaging to determine accumulation kinetics of XRCC1-YFP in CSB-proficient (upper panel) or CSB-deficient (lower panel) MRC-5 cells on BER induced SSBs cells at micro-irradiated (405 nm laser) subnuclear regions, indicated by arrows, in the presence of 10 μM Ro 19-8022 photosensitizer and 15 μM PJ-34. (**D**) Accumulation kinetics of XRCC1-YFP on BER induced SSBs (as shown in C). The mean relative fluorescence intensity is plotted against time in seconds. (**E**) Representative stills of time-lapse imaging to determine accumulation kinetics of the XRCC1^{L360D}-YFP mutant in CSB-proficient (upper panel) or CSB-deficient (lower panel) MRC-5 cells at micro-irradiated (405 nm laser) subnuclear regions, indicated by arrows. (**F**) Accumulation kinetics of the XRCC1^{L360D}-YFP mutant at micro-irradiated areas (as shown in E). The mean relative fluorescence intensity is plotted against time in seconds. (**G**) Representative stills of time-lapse imaging to determine accumulation kinetics of the XRCC1^{L360D}-YFP mutant in CSB-proficient (upper panel) or CSB-deficient (lower panel) MRC-5 cells at micro-irradiated (405 nm laser) subnuclear regions, indicated by arrows, in the presence of 10 μM Ro 19-8022 photosensitizer. (**H**) Accumulation kinetics of the XRCC1^{L360D}-YFP mutant at micro-irradiated areas (as shown in G). The mean relative fluorescence intensity is plotted against time in seconds. For (A, C, E and F), scale bar: 7.5 μm. For (B, D, F and H), error bars indicate the SEM of 20 cells of two independent, pooled experiments.

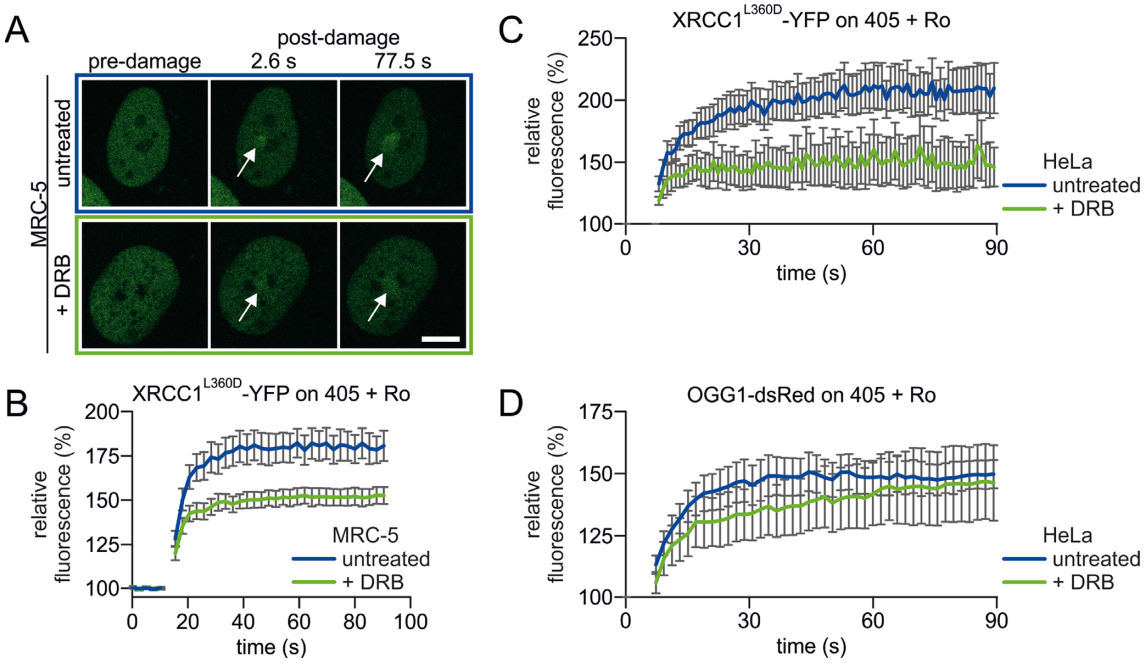

Figure 3. XRCC1 binding to BER induced breaks is sensitive to inhibition of transcription. (**A**) Representative stills of time-lapse imaging to determine accumulation kinetics of XRCC1^{L360D}-YFP in untreated (upper panel) or transcription inhibited (DRB, 100 μM) MRC-5 cells at micro-irradiated (405 nm laser) subnuclear regions, indicated by arrows, in the presence of 10 μM Ro 19-8022 photosensitizer. Scale bar: 7.5 μm. (**B**) Accumulation kinetics of XRCC1^{L360D}-YFP at micro-irradiated areas (as shown in A). The mean relative fluorescence intensity is plotted against time in seconds. Error bars indicate the SEM of 20 cells of 2 independent, pooled experiments. (**C**) Accumulation kinetics of XRCC1^{L360D}-YFP expressed in HeLa cells at micro-irradiated areas in the presence of 5 μM Ro 19-8022 photosensitizer in either untreated cells or in the presence of transcription inhibitor (DRB, 100 μM). (**D**) Accumulation kinetics of OGG1-dsRed expressed in HeLa cells at micro-irradiated areas in the presence of 5 μM Ro 19-8022 photosensitizer in either untreated cells or in the presence of transcription inhibition (DRB, 100 μM). All graphs are representative for two independent experiments (at least 11 cells) and show the mean relative fluorescence intensity ± SEM.

study (18) that overexpression of OGG1 (assumed to create more BER-intermediates) caused a stronger accumulation of XRCC1L360D at local oxidative DNA damage, strongly supports our model. Indeed, earlier studies have shown that these BER-intermediates do stall RNAPII (29–31,49). Our findings support the concept that elongating RNAPII, by virtue of its DNA-translocating activity, scans DNA for perturbations, either bulky lesions or BER-intermediates (50). It is thus likely that CSB comes into play at these BER-intermediate stalled RNAPII complexes, similarly as to its role in TC-NER. Stalled RNAPII complexes at BER-intermediates will likely disturb efficient progression of the BER reaction as the presence of these bulky molecular complexes may hamper efficient loading of downstream factors (DNA polymerase β or the ligase complex).

Different functions for CSB in TC-NER have been proposed, ranging from: being a chromatin-remodeling factor, or a recruitment platform for downstream NER factors, to pushing back or facilitating ubiquitylation and subsequent degradation of stalled RNAPII complexes to provide more efficient access of NER factors (23). The exact role of CSB in facilitating BER needs to be determined, similarly to its still enigmatic role in TC-NER. It is possible that the proposed chromatin-remodeling function of CSB, in addition to its role in coordinating TC-NER, may create a permissive chromatin environment to enable better access to repair factors. Recently, evidence has accumulated that indeed chromatin reorganization is strongly associated to TC-NER (33,51–53). Strikingly, in addition to a role of FACT in stimulating transcription restart in conjunction to TC-NER (33), also a role of FACT in facilitating BER was established (32). In our model we propose that transcription (when stalled at repair-intermediates) interferes with optimal recruitment or loading of downstream BER factors. It is thus conceivable that a BER-coordinating process is operational to prevent a clash between transcription and BER. The observed relocation of the BER machinery, including XRCC1 and Ligase3 to euchromatic (transcriptional active) regions in response to oxidative stress, might reflect such a mechanism to stimulate BER-efficiency in these regions to avoid interference with transcription (18,20,39). The compromised progression of the BER reaction due to interference with stalled transcription complexes on reaction intermediates, suggests a joint role for CSB and XRCC1 in coordinating this specific BER reaction. In addition to a pivotal organizing role for XRCC1 in SSB repair (44,54), it seems also important in coordinating BER reactions that are confronted with stalled RNAPII, likely through its scaffolding function and multiple established interactions with BER factors. BER-intermediates that are (partly) shielded by stalled transcription complexes may need CSB to help a rapid loading of XRCC1. BER coordination, mediated by XRCC1, may become more important under specific circumstances, such as in transcribed genes, on lesions that are difficult to process, or at specific genomic loci or chromatin compaction-status that hamper efficient BER pro-

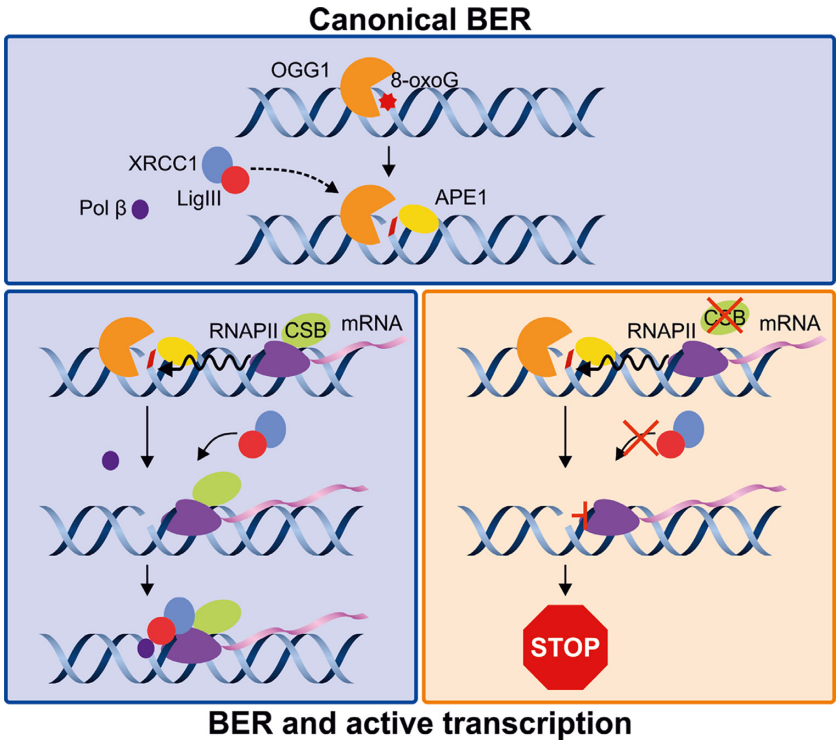

Figure 4. Proposed model for the CSB function in the repair of oxidative DNA damage. The upper panel represents the classical BER initiation on 8-oxoG lesions (red star) by the concerted action of the OOG1 glycosylase (orange sphere) and APE1 (yellow ball), subsequent recruitment of the XRCC1/LigaseIII complex (blue and red balls, respectively) and DNA Polymerase β (Pol β, dark purple ball) through interaction with the glycosylase further completes repair. The lower panels represent a situation in which an elongating RNA polymerase II complex (RNAPII, purple sphere, direction indicated by curved arrow) runs into a BER-intermediate (e.g. BER-generated SSB) that likely caused inhibition of RNAPII elongation. When CSB (green ball) is present (lower left panel, blue shaded) it will assist in loading the XRCC1/Ligase III (LigIII) complex (blue and red balls, respectively) to stalled RNAPII on BER-intermediates to facilitate the assembly of downstream BER factors, such as DNA Polymerase β (Pol β, dark-purple ball) and stimulate BER progression. In the absence of CSB (lower right panel, orange shaded), BER progression will be limited.

gression (50). CSB may be required for efficient loading of XRCC1, possibly by restructuring the stalled transcription machinery to allow exposure of glycosylase-generated intermediates. Strikingly, active parylation is not required for the recruitment of XRCC1 to BER-intermediate-stalled transcription complexes, whereas parylation is essential for loading to BER-unrelated SSBs. These observations do however not preclude a role of parylation in further downstream BER events, which was suggested previously (55).

SUPPLEMENTARY DATA

Supplementary Data are available at NAR Online.

ACKNOWLEDGEMENTS

We thank Mirjam Steur and Dimitar Angelov for assistance with some of the experiments and technical support, the Optical Imaging Centre (OIC) of the Erasmus MC for microscopy support, the ENS imaging platform (PLATIM), the IFR128 for technical support.

FUNDING

Marie Curie grant [PIEF-GA-254858 to H.M.]; Ligue Nationale contre le Cancer post-doc support to H.M.; Dutch Organization for Scientific Research [ZonMW-TOP 912.12.132 to W.V., Horizon-Zenith 935.11.042 and VIDI-ALW 864.13.004 to J.A.M.]; European Research Council Advanced Grant [340988-ERC-ID to W.V.]; Erasmus MC fellowship (to J.A.M.); Association pour la Recherche sur le Cancer [PJ20151203141 to J.P.R., A.C.]. Funding for open access charge: European Research Council Advanced Grant.
Conflict of interest statement. None declared.

REFERENCES

1. Hoeijmakers,J.H. (2009) DNA damage, aging, and cancer. *N. Engl. J. Med.*, **361**, 1475–1485.
2. Wallace,S.S. (2014) Base excision repair: a critical player in many games. *DNA Repair (Amst.)*, **19**, 14–26.
3. Cadet,J., Douki,T. and Ravanat,J.L. (2011) Measurement of oxidatively generated base damage in cellular DNA. *Mutat. Res.*, **711**, 3–12.
4. Shibutani,S., Takeshita,M. and Grollman,A.P. (1991) Insertion of specific bases during DNA synthesis past the oxidation-damaged base 8-oxodG. *Nature*, **349**, 431–434.
5. Radicella,J.P., Dherin,C., Desmaze,C., Fox,M.S. and Boiteux,S. (1997) Cloning and characterization of hOGG1, a human homolog of the OGG1 gene of Saccharomyces cerevisiae. *Proc. Natl. Acad. Sci. U.S.A.*, **94**, 8010–8015.
6. Izumi,T., Hazra,T.K., Boldogh,I., Tomkinson,A.E., Park,M.S., Ikeda,S. and Mitra,S. (2000) Requirement for human AP endonuclease 1 for repair of 3′-blocking damage at DNA single-strand breaks induced by reactive oxygen species. *Carcinogenesis*, **21**, 1329–1334.

7. Vidal,A.E., Boiteux,S., Hickson,I.D. and Radicella,J.P. (2001) XRCC1 coordinates the initial and late stages of DNA abasic site repair through protein-protein interactions. *EMBO J.*, **20**, 6530–6539.
8. Wilson,D.M. and Thompson,L.H. (1997) Life without DNA repair. *Proc. Natl. Acad. Sci. U.S.A.*, **94**, 12754–12757.
9. Marsin,S., Vidal,A.E., Sossou,M., Menissier-de Murcia,J., Le Page,F., Boiteux,S., de Murcia,G. and Radicella,J.P. (2003) Role of XRCC1 in the coordination and stimulation of oxidative DNA damage repair initiated by the DNA glycosylase hOGG1. *J. Biol. Chem.*, **278**, 44068–44074.
10. Caldecott,K.W. (2003) XRCC1 and DNA strand break repair. *DNA Repair (Amst.)*, **2**, 955–969.
11. Caldecott,K.W. (2007) Mammalian single-strand break repair: mechanisms and links with chromatin. *DNA Repair (Amst.)*, **6**, 443–453.
12. Hanzlikova,H., Gittens,W., Krejcikova,K., Zeng,Z. and Caldecott,K.W. (2017) Overlapping roles for PARP1 and PARP2 in the recruitment of endogenous XRCC1 and PNKP into oxidized chromatin. *Nucleic Acids Res.*, **45**, 2546–2557.
13. Pascucci,B., Maga,G., Hubscher,U., Bjoras,M., Seeberg,E., Hickson,I.D., Villani,G., Giordano,C., Cellai,L. and Dogliotti,E. (2002) Reconstitution of the base excision repair pathway for 7,8-dihydro-8-oxoguanine with purified human proteins. *Nucleic.Acids Res.*, **30**, 2124–2130.
14. Kubota,Y., Nash,R.A., Klungland,A., Schar,P., Barnes,D.E. and Lindahl,T. (1996) Reconstitution of DNA base excision-repair with purified human proteins: interaction between DNA polymerase beta and the XRCC1 protein. *EMBO J.*, **15**, 6662–6670.
15. Menoni,H., Gasparutto,D., Hamiche,A., Cadet,J., Dimitrov,S., Bouvet,P. and Angelov,D. (2007) ATP-dependent chromatin remodeling is required for base excision repair in conventional but not in variant H2A.Bbd nucleosomesv. *Mol. Cell. Biol.*, **27**, 5949–5956.
16. Menoni,H., Shukla,M.S., Gerson,V., Dimitrov,S. and Angelov,D. (2012) Base excision repair of 8-oxoG in dinucleosomes. *Nucleic Acids Res.*, **40**, 692–700.
17. Odell,I.D., Barbour,J.E., Murphy,D.L., Della-Maria,J.A., Sweasy,J.B., Tomkinson,A.E., Wallace,S.S. and Pederson,D.S. (2011) Nucleosome disruption by DNA ligase III-XRCC1 promotes efficient base excision repair. *Mol. Cell. Biol.*, **31**, 4623–4632.
18. Campalans,A., Kortulewski,T., Amouroux,R., Menoni,H., Vermeulen,W. and Radicella,J.P. (2013) Distinct spatiotemporal patterns and PARP dependence of XRCC1 recruitment to single-strand break and base excision repair. *Nucleic Acids Res.*, **41**, 3115–3129.
19. Campalans,A., Marsin,S., Nakabeppu,Y., O'Connor,T.R., Boiteux,S. and Radicella,J.P. (2005) XRCC1 interactions with multiple DNA glycosylases: a model for its recruitment to base excision repair. *DNA Repair (Amst.)*, **4**, 826–835.
20. Campalans,A., Moritz,E., Kortulewski,T., Biard,D., Epe,B. and Radicella,J.P. (2015) Interaction with OGG1 is required for efficient recruitment of XRCC1 to base excision repair and maintenance of genetic stability after exposure to oxidative stress. *Mol. Cell. Biol.*, **35**, 1648–1658.
21. Strom,C.E., Johansson,F., Uhlen,M., Szigyarto,C.A., Erixon,K. and Helleday,T. (2011) Poly (ADP-ribose) polymerase (PARP) is not involved in base excision repair but PARP inhibition traps a single-strand intermediate. *Nucleic Acids Res.*, **39**, 3166–3175.
22. Menoni,H., Hoeijmakers,J.H. and Vermeulen,W. (2012) Nucleotide excision repair-initiating proteins bind to oxidative DNA lesions in vivo. *J. Cell Biol.*, **199**, 1037–1046.
23. Marteijn,J.A., Lans,H., Vermeulen,W. and Hoeijmakers,J.H. (2014) Understanding nucleotide excision repair and its roles in cancer and ageing. *Nat. Rev. Mol. Cell. Biol.*, **15**, 465–481.
24. Dianov,G., Bischoff,C., Sunesen,M. and Bohr,V.A. (1999) Repair of 8-oxoguanine in DNA is deficient in Cockayne syndrome group B cells. *Nucleic Acids Res.*, **27**, 1365–1368.
25. Osterod,M., Larsen,E., Le Page,F., Hengstler,J.G., Van Der Horst,G.T., Boiteux,S., Klungland,A. and Epe,B. (2002) A global DNA repair mechanism involving the Cockayne syndrome B (CSB) gene product can prevent the in vivo accumulation of endogenous oxidative DNA base damage. *Oncogene*, **21**, 8232–8239.
26. Stevnsner,T., Muftuoglu,M., Aamann,M.D. and Bohr,V.A. (2008) The role of Cockayne Syndrome group B (CSB) protein in base excision repair and aging. *Mech. Ageing Dev.*, **129**, 441–448.
27. Tuo,J., Chen,C., Zeng,X., Christiansen,M. and Bohr,V.A. (2002) Functional crosstalk between hOgg1 and the helicase domain of Cockayne syndrome group B protein. *DNA Repair (Amst.)*, **1**, 913–927.
28. Singh,S.K., Szulik,M.W., Ganguly,M., Khutsishvili,I., Stone,M.P., Marky,L.A. and Gold,B. (2011) Characterization of DNA with an 8-oxoguanine modification. *Nucleic Acids Res.*, **39**, 6789–6801.
29. Kathe,S.D., Shen,G.P. and Wallace,S.S. (2004) Single-stranded breaks in DNA but not oxidative DNA base damages block transcriptional elongation by RNA polymerase II in HeLa cell nuclear extracts. *J. Biol. Chem.*, **279**, 18511–18520.
30. Khobta,A., Kitsera,N., Speckmann,B. and Epe,B. (2009) 8-Oxoguanine DNA glycosylase (Ogg1) causes a transcriptional inactivation of damaged DNA in the absence of functional Cockayne syndrome B (Csb) protein. *DNA Repair (Amst.)*, **8**, 309–317.
31. Kitsera,N., Stathis,D., Luhnsdorf,B., Muller,H., Carell,T., Epe,B. and Khobta,A. (2011) 8-Oxo-7,8-dihydroguanine in DNA does not constitute a barrier to transcription, but is converted into transcription-blocking damage by OGG1. *Nucleic Acids Res.*, **39**, 5926–5934.
32. Charles Richard,J.L., Shukla,M.S., Menoni,H., Ouararhni,K., Lone,I.N., Roulland,Y., Papin,C., Ben Simon,E., Kundu,T., Hamiche,A. *et al.* (2016) FACT assists base excision repair by boosting the remodeling activity of RSC. *PLoS Genet.*, **12**, e1006221.
33. Dinant,C., Ampatziadis-Michailidis,G., Lans,H., Tresini,M., Lagarou,A., Grosbart,M., Theil,A.F., van Cappellen,W.A., Kimura,H., Bartek,J. *et al.* (2013) Enhanced chromatin dynamics by FACT promotes transcriptional restart after UV-induced DNA damage. *Mol. Cell*, **51**, 469–479.
34. Sanjana,N.E., Shalem,O. and Zhang,F. (2014) Improved vectors and genome-wide libraries for CRISPR screening. *Nat. Methods*, **11**, 783–784.
35. Campeau,E., Ruhl,V.E., Rodier,F., Smith,C.L., Rahmberg,B.L., Fuss,J.O., Campisi,J., Yaswen,P., Cooper,P.K. and Kaufman,P.D. (2009) A versatile viral system for expression and depletion of proteins in mammalian cells. *PLoS One*, **4**, e6529.
36. van Cuijk,L., van Belle,G.J., Turkyilmaz,Y., Poulsen,S.L., Janssens,R.C., Theil,A.F., Sabatella,M., Lans,H., Mailand,N., Houtsmuller,A.B. *et al.* (2015) SUMO and ubiquitin-dependent XPC exchange drives nucleotide excision repair. *Nat. Commun.*, **6**, 7499.
37. Garcia Soriano,F., Virag,L., Jagtap,P., Szabo,E., Mabley,J.G., Liaudet,L., Marton,A., Hoyt,D.G., Murthy,K.G., Salzman,A.L. *et al.* (2001) Diabetic endothelial dysfunction: the role of poly(ADP-ribose) polymerase activation. *Nat. Med.*, **7**, 108–113.
38. Bensaude,O. (2011) Inhibiting eukaryotic transcription: Which compound to choose? How to evaluate its activity? *Transcription*, **2**, 103–108.
39. Amouroux,R., Campalans,A., Epe,B. and Radicella,J.P. (2010) Oxidative stress triggers the preferential assembly of base excision repair complexes on open chromatin regions. *Nucleic Acids Res.*, **38**, 2878–2890.
40. Ropolo,M., Degan,P., Foresta,M., D'Errico,M., Lasiglie,D., Dogliotti,E., Casartelli,G., Zupo,S., Poggi,A. and Frosina,G. (2007) Complementation of the oxidatively damaged DNA repair defect in Cockayne syndrome A and B cells by Escherichia coli formamidopyrimidine DNA glycosylase. *Free Radic. Biol. Med.*, **42**, 1807–1817.
41. Guo,J., Hanawalt,P.C. and Spivak,G. (2013) Comet-FISH with strand-specific probes reveals transcription-coupled repair of 8-oxoGuanine in human cells. *Nucleic Acids Res.*, **41**, 7700–7712.
42. Kong,X., Mohanty,S.K., Stephens,J., Heale,J.T., Gomez-Godinez,V., Shi,L.Z., Kim,J.S., Yokomori,K. and Berns,M.W. (2009) Comparative analysis of different laser systems to study cellular responses to DNA damage in mammalian cells. *Nucleic Acids Res.*, **37**, e68.
43. Lan,L., Nakajima,S., Oohata,Y., Takao,M., Okano,S., Masutani,M., Wilson,S.H. and Yasui,A. (2004) In situ analysis of repair processes for oxidative DNA damage in mammalian cells. *Proc. Natl. Acad. Sci. U.S.A.*, **101**, 13738–13743.
44. El-Khamisy,S.F., Masutani,M., Suzuki,H. and Caldecott,K.W. (2003) A requirement for PARP-1 for the assembly or stability of XRCC1 nuclear foci at sites of oxidative DNA damage. *Nucleic Acids Res.*, **31**, 5526–5533.

45. Charlet-Berguerand,N., Feuerhahn,S., Kong,S.E., Ziserman,H., Conaway,J.W., Conaway,R. and Egly,J.M. (2006) RNA polymerase II bypass of oxidative DNA damage is regulated by transcription elongation factors. *EMBO J.*, **25**, 5481–5491.
46. Steurer,B. and Marteijn,J.A. (2016) Traveling rocky roads: the consequences of transcription-blocking DNA lesions on RNA polymerase II. *J. Mol. Biol.*, **429**, 3146–3155
47. Nazarkina,Z.K., Khodyreva,S.N., Marsin,S., Lavrik,O.I. and Radicella,J.P. (2007) XRCC1 interactions with base excision repair DNA intermediates. *DNA Repair (Amst.)*, **6**, 254–264.
48. Klungland,A., Rosewell,I., Hollenbach,S., Larsen,E., Daly,G., Epe,B., Seeberg,E., Lindahl,T. and Barnes,D.E. (1999) Accumulation of premutagenic DNA lesions in mice defective in removal of oxidative base damage. *Proc. Natl. Acad. Sci. U.S.A.*, **96**, 13300–13305.
49. Tornaletti,S., Maeda,L.S., Kolodner,R.D. and Hanawalt,P.C. (2004) Effect of 8-oxoguanine on transcription elongation by T7 RNA polymerase and mammalian RNA polymerase II. *DNA Repair (Amst.)*, **3**, 483–494.
50. Menoni,H., Di Mascio,P., Cadet,J., Dimitrov,S. and Angelov,D. (2017) Chromatin associated mechanisms in base excision repair - nucleosome remodeling and DNA transcription, two key players. *Free Radic. Biol. Med.*, **107**, 159–169.
51. Adam,S., Polo,S.E. and Almouzni,G. (2013) Transcription recovery after DNA damage requires chromatin priming by the H3.3 histone chaperone HIRA. *Cell*, **155**, 94–106.
52. Aydin,O.Z., Vermeulen,W. and Lans,H. (2014) ISWI chromatin remodeling complexes in the DNA damage response. *Cell Cycle*, **13**, 3016–3025.
53. Oksenych,V., Zhovmer,A., Ziani,S., Mari,P.O., Eberova,J., Nardo,T., Stefanini,M., Giglia-Mari,G., Egly,J.M. and Coin,F. (2013) Histone methyltransferase DOT1L drives recovery of gene expression after a genotoxic attack. *PLoS Genet.*, **9**, e1003611.
54. Okano,S., Lan,L., Caldecott,K.W., Mori,T. and Yasui,A. (2003) Spatial and temporal cellular responses to single-strand breaks in human cells. *Mol. Cell. Biol.*, **23**, 3974–3981.
55. Flohr,C., Bürkle,A., Radicella,J.P. and Epe,B. (2003) Poly(ADP-ribosyl)ation accelerates DNA repair in a pathway dependent on Cockayne syndrome B protein. *Nucleic Acids Res.*, **31**, 5332–5337.